Supporting Information

Incorporation of MnO nanoparticles inside porous carbon nanotubes originated from conjugated microporous polymers for lithium storage

Qingtang Zhang,* Qinqin Dai, Meng Li, Xiaomei Wang and An Li*

State Key Laboratory of Advanced Processing and Recycling of Non-ferrous Metals, School of Petrochemical Engineering, Lanzhou University of Technology, Lanzhou, 730050, China.

CMP nanotubes were synthesized using Pd(0)/Cu(I) catalyzed Sonogashira–Hagihara crosscoupling polycondensation.

XRD analysis

Pure MnO are also prepared under the same conditions like the preparation of PCNT, MnO-PCNT and MnO-CNT. XRD patterns of pure MnO are shown in Fig. S1. The main peaks locate at 34.90, 40.54, 58.68, 70.14 and 73.76°, which can be assigned to a pure cubic phase of MnO (JCPDS Cards: 07-0230).

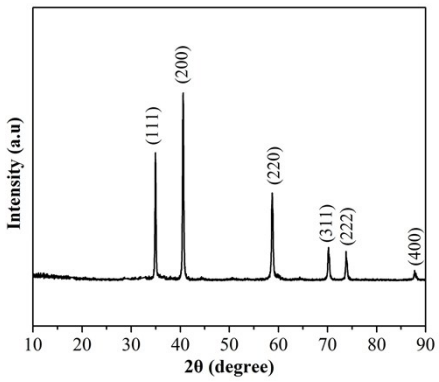

Fig S1 XRD Patterns of pure MnO

SEM analysis

Fig. S2 is the scanning electron micrograph (TEM) of the CMP nanotubes. Fig. S2(a) shows that the length of PCNT is over 10 μm. Fig. S2(b) shows that PCNT are open end tubes with diameters mainly in the range of 200~400 nm. In addition, the surface of PCNT is fairly rough and some CMP nanoparticles are on the surface of PCNT. As shown in Fig. S2c, MnO are microsized particles. These particles are composed of MnO nanoparticles about 200 nm.

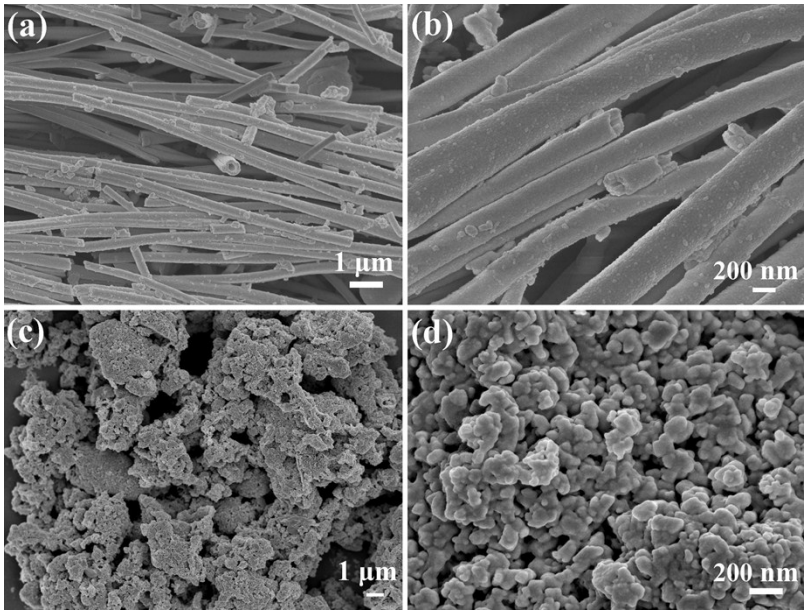

Fig. S2 (a,b) SEM images of CMP nanotubes. SEM images of MnO (c,d).

Fig. S3a is the TEM image of pure MnO. MnO are microsized particles, which are composed of nanoparticles about 200 nm. Fig. S3b clearly shows the lattice structures of MnO.

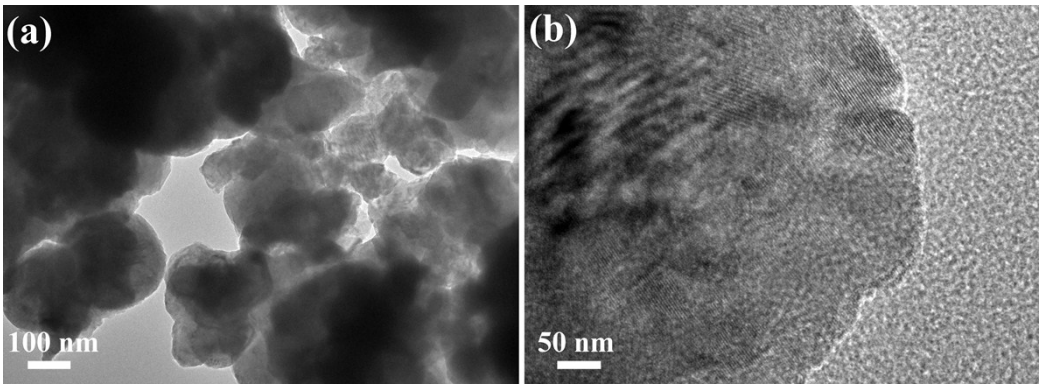

Fig. S3 TEM image of pure MnO.

Pore structure analysis

The measurements of specific surface area, pore volume, average pore size and pore distribution were performed at a Micromeritics ASAP 2020 apparatus by nitrogen adsorption and desorption isotherms at 77.3 K Specific surface areas were determined according to the Brunauer-Emmett-Teller (BET) method. The total pore volume was estimated from the amount of nitrogen adsorbed at a relative pressure of $P/P_0 = 0.99$. The pore size distribution plot was recorded from the adsorption branch

of the isotherm based on the non-local density functional theory (NLDFT) method.

The pore properties of the CMP nanotubes and pure MnO were investigated by nitrogen adsorption and desorption measurements. The obtained results are illustrated in Fig. S4. As shown in Fig. S4a, CMP nanotubes and pure MnO both displays a representative type IV isotherm, exhibiting a typical H1 hysteresis loop at moderate relative pressures (between 0.4 and 0.5 P/P_0). This indicates CMP nanotubes are mesoporous materials. The BET surface area, pore volume and average pore diameter of the sample were 10.72 m^2 g^{-1} and 0.0249 cm^3 g^{-1} and 13.7 nm, respectively. While, those for pure MnO are 0.03 m^2 g^{-1} and 0.01 cm^3 g^{-1} and 64.3 nm, respectively. Fig. S4b shows the pore distributions of CMP nanotubes and pure MnO. CMP nanotubes are typical mesoporous polymers. As shown in Fig. 4b, the pore size distribution of pure MnO are in the range of 10~255 nm. These indicate that MnO has very few macropores.

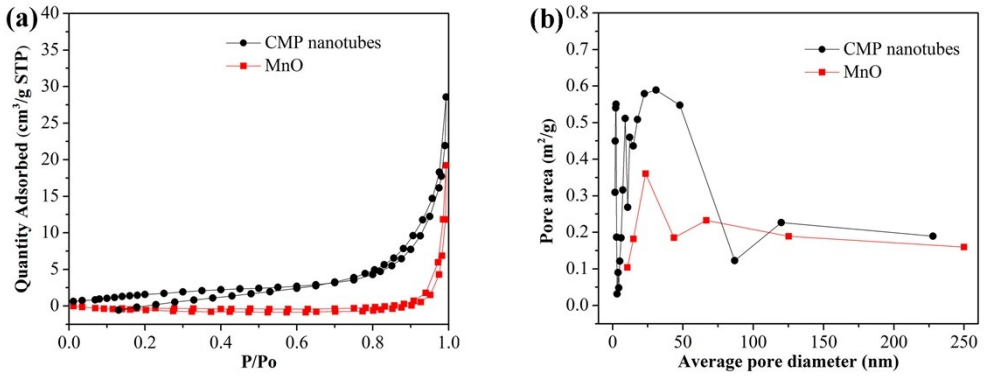

Fig. S4 Nitrogen adsorption–desorption isotherms of CMP nanotubes and pure MnO. (b) Pore distribution of CMP nanotubes and pure MnO.

The discharge-charge curves at 0.2 C within the voltage range of 0.000–3.000 V are presented in Fig. S5a,b. In the first discharge process (Fig. S5a), an obvious long voltage plateau ranging from 0.3 to 0.12 V for MnO-PCNT and MnO-CNT are related to the complete reduction of Mn^{2+} to Mn^0. The high discharge voltage plateau of MnO-PCNT means it has low electronic resistance. In the first charge process, the clear slope in the range of 1.0~1.5 V corresponds to the oxidation of Mn^0 to Mn^{2+}, which is the typical character of MnO-based electrodes. Seen from Fig. S5a, the initial discharge and charge capacities of MnO-PCNT are 933.4 and 580.4 mAh g^{-1}, while

those for MnO are 923.0 and 629.6 mAh g^{-1}. Thus, the initial columbic efficiency of MnO-PCNT and MnO-CNT are 62.2% and 68.2%. The fifth discharge-charge curves are also depicted as Fig. S5b. The fifth discharge and charge capacities of MnO are 574.9 and 562.0 mAh g^{-1}. The fifth discharge and charge capacities of MnO-PCNT are 517.0 and 502.3 mAh g^{-1}. Therefore, the fifth columbic efficiency of MnO-PCNT and MnO are 97.2% and 97.8%. The two values at fifth cycles are very close.

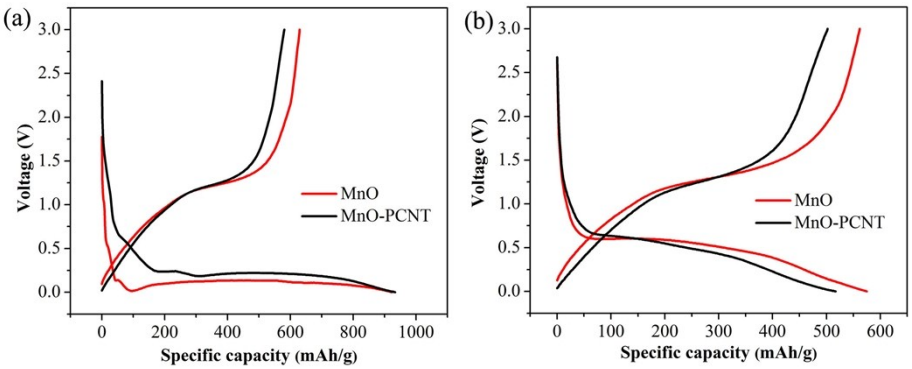

Fig. S5 Charge-discharge curves of pure MnO and MnO-PCNT.

Fig. S6 is the rate performance of MnO and Mno-PCNT. When the current rate is lower than 3 C, the charge-discharge capacities of MnO-PCNT are slightly lower than those of pure MnO. While, when the current rate is higher than 3 C, the charge-discharge capacities of MnO-PCNT are much higher than those of pure MnO. These indicate that the large rate performance of MnO-PCNT is much better than that of pure MnO.

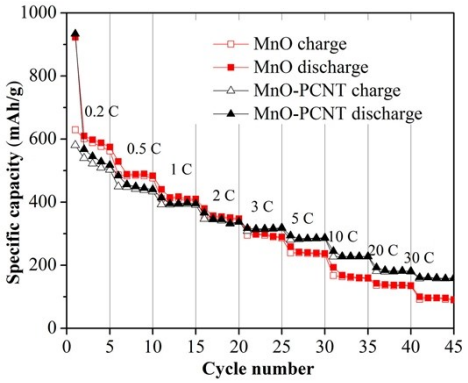

Fig. S6 Rate performance of MnO and MnO-PCNT.

The cycling performance for pure MnO and MnO-PCNT was tested at 1 C after three discharge-charge cycles activation at 0.2 C and the result are shown as Fig. S7.

Although MnO exhibits a high initial specific capacity about 500 mAh g^{-1}, the specific capacities decrease rapidly during the following cycles because of the pulverization of MnO during cycles. The 300th charge specific capacity is only 94.1 mAh g^{-1}. The capacity retention ration is 18.8%. While, for MnO-PCNT, the first and 300th reversible capacities are 409.3 and 572.6 mAh/g. The cycling stability of MnO-PCNT is much better than that of MnO.

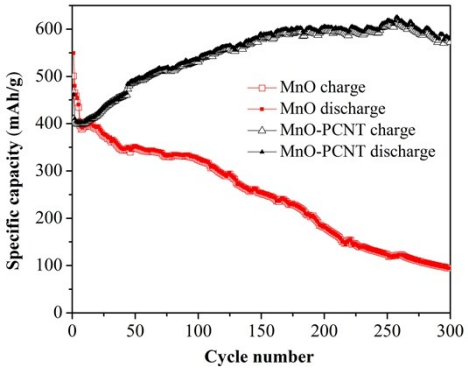

Fig. S7 Cycling performance of MnO and MnO-PCNT.

MnO-PCNT has shown excellent rate performance and cycling performance. It was further confirmed by EIS measurement. EIS of the fresh cells loaded with PCNT, MnO-PCNT and pure MnO are performed on CHI660E electrochemical station at room temperature. As shown in Fig. S8, both impedance spectra are consisted of a semicircle in high-medium frequency and a straight line in low frequency. It can be clearly observed that the charge-transfer resistance of MnO-PCNT is 173 Ω, which is much smaller than that of MnO (268 Ω).

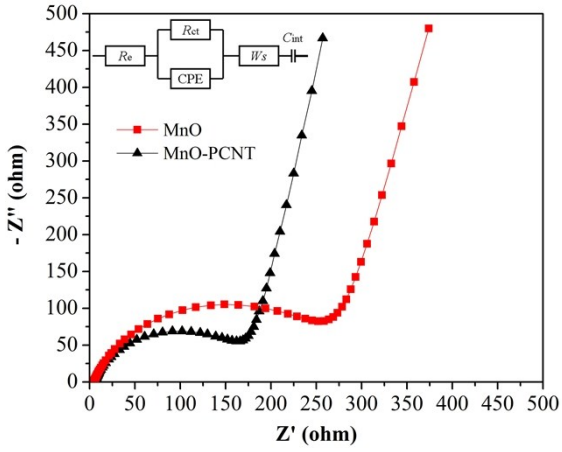

Fig. S8 EIS of the fresh cells loaded with MnO-PCNT and MnO.